Received: 11 November 2020 | Revised: 11 January 2021 | Accepted: 12 January 2021

DOI: 10.1002/pro.4025

FULL-LENGTH PAPERS

THE PROTEIN SOCIETY WILEY

Interplay between tau and α-synuclein liquid–liquid phase separation

Anna Siegert[1] | **Marija Rankovic**[2] | **Filippo Favretto**[1] | **Tina Ukmar-Godec**[1] | **Timo Strohäker**[1] | **Stefan Becker**[2] | **Markus Zweckstetter**[1,2]

[1]German Center for Neurodegenerative Diseases (DZNE), Göttingen, Germany

[2]Department for NMR-based Structural Biology, Max Planck Institute for Biophysical Chemistry, Göttingen, Germany

Correspondence
Markus Zweckstetter, German Center for Neurodegenerative Diseases (DZNE), Von-Siebold-Str. 3a, 37075 Göttingen, Germany.
E-mail: markus.zweckstetter@dzne.de

Funding information
H2020 European Research Council, Grant/Award Number: 787679 - LLPS-NMR; Michael J. Fox Foundation for Parkinson's Research, Grant/Award Number: 16075

Abstract

In Parkinson's disease with dementia, up to 50% of patients develop a high number of tau-containing neurofibrillary tangles. Tau-based pathologies may thus act synergistically with the α-synuclein pathology to confer a worse prognosis. A better understanding of the relationship between the two distinct pathologies is therefore required. Liquid–liquid phase separation (LLPS) of proteins has recently been shown to be important for protein aggregation involved in amyotrophic lateral sclerosis, whereas tau phase separation has been linked to Alzheimer's disease. We therefore investigated the interaction of α-synuclein with tau and its consequences on tau LLPS. We find α-synuclein to have a low propensity for both, self-coacervation and RNA-mediated LLPS at pH 7.4. However, full-length but not carboxy-terminally truncated α-synuclein efficiently partitions into tau/RNA droplets. We further demonstrate that Cdk2-phosphorylation promotes the concentration of tau into RNA-induced droplets, but at the same time decreases the amount of α-synuclein inside the droplets. NMR spectroscopy reveals that the interaction of the carboxy-terminal domain of α-synuclein with the proline-rich region P2 of tau is required for the recruitment of α-synuclein into tau droplets. The combined data suggest that the concentration of α-synuclein into tau-associated condensates can contribute to synergistic aSyn/tau pathologies.

KEYWORDS

LLPS, phosphorylation, tau, truncation, α-synuclein

Abbreviations: aSyn, α-synuclein; $aSyn^{\Delta C}$, residue 1–107 of α-synuclein; DIC, differential interference contrast microscopy; DTT, dithiothreitol; FRAP, fluorescence recovery after photobleaching; FUS, fused in sarcoma; HEPES, 2-(4-[2-hydroxyethyl]-1-piperazinyl)-ethansulfonsäure; HMQC, heteronuclear multiple quantum coherence; K_d, dissociation constant; LD, liquid-like droplet; LLPS, liquid–liquid phase separation; MHz, megahertz; NMR, nuclear magnetic resonance; PBS, phosphate buffered saline; PDD, Parkinson's disease with dementia; PEG, polyethylene glycol; PolyU, polyuridylic acid; pTau(Cdk2), tau phosphorylated by Cdk2; RNA, ribonucleic acid.

1 | INTRODUCTION

In Parkinson's disease with dementia (PDD), up to 50% of patients develop a high number of tau-containing neurofibrillary tangles, and these pathologies may act synergistically with α-synuclein (aSyn) pathology to confer a worse prognosis.[1,2] aSyn and tau filamentous inclusions also co-occur in transgenic mice.[3] In vitro, aSyn induces fibrillization of tau. Coincubation of tau and aSyn synergistically promotes oligomerization and fibrillization of both proteins.[3,4] In addition, tau enhances aSyn aggregation and toxicity in cellular models of synucleinopathies.[5] Oligomers of aSyn and tau exist in the same aggregates, forming hybrid oligomers in the brains of Parkinson's disease patients.[6] aSyn can directly bind to tau[7-9] and interactions between aSyn and tau augment neurotoxicity in a drosophila model of Parkinson's disease.[10] The importance of synergistic aggregation of aSyn and tau is further supported by the observation that distinct aSyn strains assembled in vitro differentially promote tau inclusions in neurons.[11] A better understanding of the relationships between these two distinct pathologies is therefore required for the development of effective disease-modifying treatments for PDD.[1,2]

An increasing role in neurodegeneration is attributed to liquid–liquid phase separation (LLPS) of low complexity regions and intrinsically disordered proteins.[12-14] For example, the low complexity domain-containing protein fused in sarcoma (FUS) undergoes LLPS prior to conversion into insoluble deposits.[15] Insoluble deposits of FUS are found in the brains of patients with Pick's disease and frontotemporal dementias.[16] Disease mutations in FUS leading to amyotrophic lateral sclerosis accelerate the transition from the liquid demixed state to an aberrant aggregated form,[15] while phosphorylation interferes with LLPS of the FUS low-complexity region.[17] In addition, toxic dipeptide repeats coded by hexanucleotide expansions in the *C9ORF72* gene, which are major causes of familial amyotrophic lateral sclerosis and frontotemporal dementia, condense to form liquid droplets.[18] Other proteins associated with amyotrophic lateral sclerosis, such as hnRNPA1 and TDP43, also separate into distinct phases in solution.[19,20]

Tau has a strong propensity for LLPS in vitro,[21-23] with heparin-induced fibrillization of tau being strongest in buffer conditions that promote tau LLPS such as low ionic strength and physiological temperature.[21] Posttranslational modifications modulate tau LLPS: phosphorylation promotes tau LLPS,[21,23,24] while acetylation blocks tau LLPS in vitro[25,26] as well as co-localization of tau with stress granules in cells.[26] LLPS of tau also provides a mechanism for the concentration of tubulin inside tau droplets resulting in highly efficient assembly of tau into microtubules,[27] a process that is blocked by phosphorylation of tau at the disease-associated epitope AT180.[24] In addition, tau forms condensates on the surface of microtubules.[28,29] Moreover, it was recently shown that aSyn can undergo LLPS at low pH.[30]

Here we study the ability of full-length and C-terminally truncated aSyn to undergo LLPS alone or in the presence of RNA and to concentrate inside of preformed tau droplets. We also investigate whether the recruitment of aSyn affects the diffusion of tau inside droplets and determine the residue-specific basis for the interaction between tau and aSyn, which determines the enrichment of aSyn inside tau droplets.

2 | RESULTS

2.1 | aSyn and aSyn$^{\Delta C}$ do not phase separate at pH 7.4

To investigate the ability of the Parkinson's disease-associated protein aSyn to undergo LLPS in vitro, we recombinantly produced full-length human aSyn (140 residues). Because C-terminally truncated versions of aSyn are present in the brains of Parkinson's disease patients,[31,32] we also prepared aSyn$^{\Delta C}$ comprising residues 1–107 of aSyn.

Using differential interference contrast (DIC) microscopy as well as fluorescence microscopy, a range of different sample conditions was screened for LLPS of the two proteins (Table S1). The experiments were performed at pH 7.4 with aSyn concentrations up to 500 μM, that is, at least 10-fold higher than aSyn concentrations in neurons. In addition, different buffers (PBS and HEPES) were tested, as well as the two molecular crowding agents dextran and polyethylene glycol (PEG). No protein droplets were detected under any of these conditions (Figure S1, Table S1). The combined experiments showed that full-length aSyn does not undergo LLPS in these conditions, in agreement with a low propensity of aSyn for LLPS at pH 7.4.[30] In addition, the experiments showed that the removal of the negatively charged C-terminal domain of aSyn does not promote LLPS under these conditions.

2.2 | RNA fails to promote aSyn or aSyn$^{\Delta C}$ phase separation

Next, we tested the propensity of aSyn for cooperative LLPS with nucleic acids. This type of LLPS is known as complex coacervation. Indeed, many proteins were shown to undergo complex coacervation with RNA, in agreement with the observation of biomolecular condensates in cells that are rich in RNA.[33,34] Using different molar ratios of

aSyn and tRNA, LLPS was probed at 37°C using both DIC and fluorescence microscopy. Under none of the conditions, however, LLPS was detected (Table S2). In addition, we performed DIC experiments for $aSyn^{\Delta C}$ (100 μM) in the presence of different concentrations of polyU RNA (0.05–1.5 mg/ml). Again, no droplets, which would suggest the occurrence of LLPS, were observed (Table S2). The experiments showed that aSyn has a low propensity for RNA-mediated phase separation under these conditions.

2.3 | aSyn concentrates inside tau droplets

Besides the ability of aSyn to undergo LLPS in solution, a potential role for LLPS in the pathogenic misfolding of aSyn could reside in the recruitment of aSyn to phase-separated compartments formed by other proteins. Because of the known synergistic role of aSyn and tau in the proteins' aggregation,[1-11] we investigated if aSyn concentrates into preformed droplets of tau (Figure 1a).

To this end, we recombinantly produced the 441-residue 2N4R tau (further termed tau), the longest isoform of tau in the adult human brain.[35] Previous studies had shown that tau phase separates efficiently using RNA,[22,26] in agreement with the ability of tau to co-localize with stress granules,[26,36] cellular condensates rich in RNA. We therefore formed droplets by mixing tau (50 μM) with polyU RNA (60 nM). To increase the stability of the droplets, we additionally added 2.5% dextran.[26] Tau protein strongly concentrated inside the droplets (Table 1). In addition, we prepared tau droplets in the

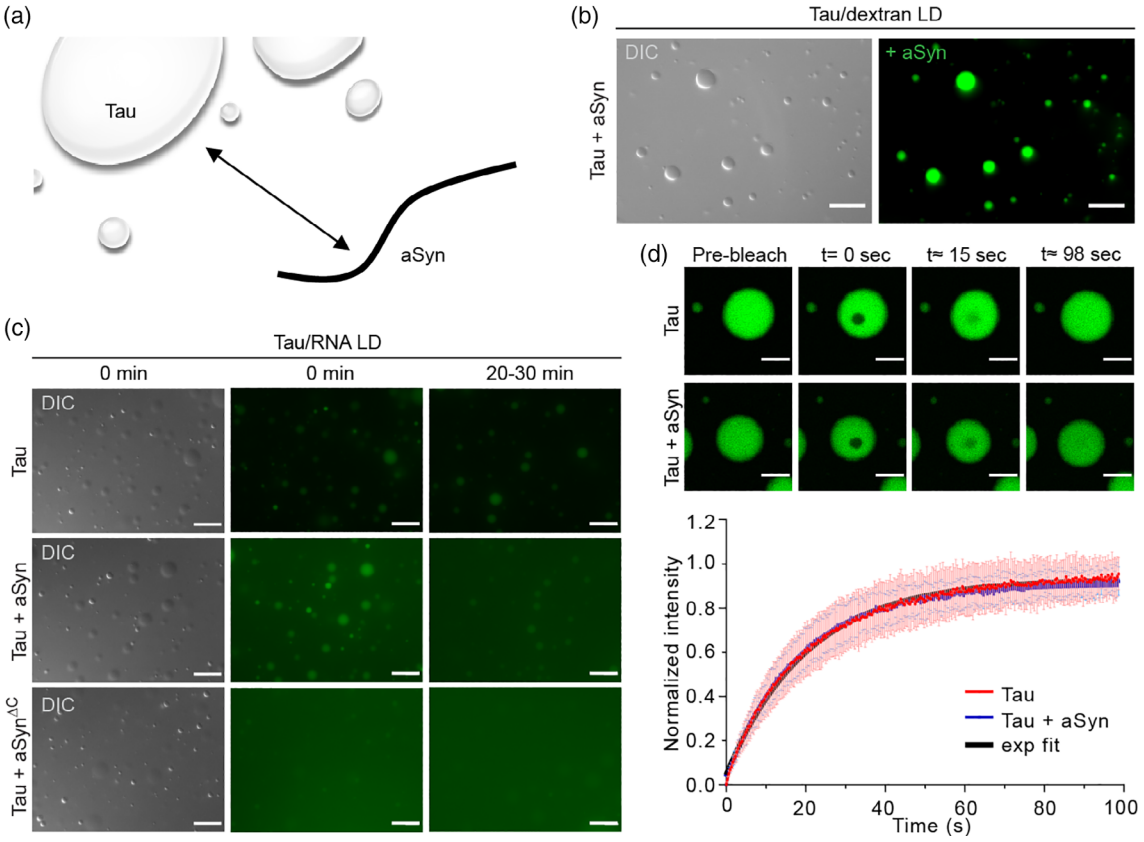

FIGURE 1 aSyn recruitment into phase-separated liquid-like droplets of tau protein. (a) Schematic representation of aSyn recruitment into tau droplets. (b) Differential interference contrast microscopy (DIC) and fluorescence microscopy demonstrate strong concentration of fluorescein (FAM)-labeled aSyn (2 μM; green channel) in tau liquid-like droplets (LD) formed by LLPS in the presence of 10% dextran (tau/dextran LD). (c) Tau/RNA liquid droplets (tau/RNA LD) of tau protein alone (60 μM, spiked with small amount of Alexa Fluor 488-labeled tau) or tau protein (50 μM) in combination with aSyn or $aSyn^{\Delta C}$ proteins (10 μM, spiked with small amount of Alexa Fluor 488-labeled aSyn or $aSyn^{\Delta C}$, respectively) were formed using 60 nM polyU and stabilized by addition of 2.5% dextran. Liquid droplets were imaged immediately (0 min) or after 20–30 min of incubation at room temperature. (d) Normalized mean FRAP recovery curves and corresponding FRAP images of 60 μM tau control sample (red curve; upper panels) and 50 μM tau +10 μM aSyn sample (blue curve; lower panels). Tau or tau + aSyn liquid droplets were prepared using 60 nM polyU and 2.5% dextran as described in Section 4 and spiked with a small amount of Alexa Fluor 488-labeled tau. Data points represent mean values across five replicates and error bars show ± *SD*. Fitting of data (black curves) was done assuming an exponential recovery. FRAP images show pre-bleached sample (pre-bleach), bleached sample ($t = 0$), and sample after $t \approx 15$ s or $t \approx 98$ s of recovery. Scale bars, 20 μm in (b) and (c), and 10 μm in (d)

TABLE 1 Partitioning coefficients of fluorescently labeled tau, aSyn or aSyn$^{\Delta C}$ into tau/RNA or pTau(Cdk2)/RNA droplets

	Tau/RNA LDs	pTau(Cdk2)/RNA LDs
Tau	3.26 ± 0.41	4.46 ± 0.49
aSyn	1.83 ± 0.29	1.21 ± 0.04
aSyn$^{\Delta C}$	1.05 ± 0.05	1.03 ± 0.01

Note: Liquid droplets of tau control (tau/RNA LDs) or Cdk2-phosphorylated tau (pTau(Cdk2)/RNA LDs) were prepared using 60 nM polyU and 2.5% dextran as described in the Section 4. Partitioning coefficients of fluorescently labeled tau, aSyn or aSyn$^{\Delta C}$ were calculated as the average droplet fluorescence intensity over the average fluorescence intensity of the dispersed phase (background) and presented as a mean ± *SD* of 60–70 droplets/background measurements from two independent experiments.

absence of RNA by increasing the concentration of dextran to 10% dextran (Figure 1b).

We then added 10 μM of aSyn to the preformed tau droplets such that the tau concentration was fivefold higher when compared to aSyn. aSyn alone did not form droplets (Figure S1). Fluorescence microscopy showed that aSyn concentrates inside the tau droplets independent of the presence of RNA (Figure 1b,c, respectively). Comparison of the fluorescence intensity of aSyn inside and outside of the tau/RNA droplets yielded a partition coefficient of 1.83 ± 0.29 (Table 1). In contrast, the concentration of the C-terminally truncated aSyn did not increase inside tau/RNA droplets (Figure 1c, bottom row; Table 1).

2.4 | Rapid tau diffusion in tau/RNA/aSyn droplets

Next, we asked if the recruitment of aSyn into tau/RNA droplets modulates the intra-droplet diffusion of tau. The latter was examined by fluorescence recovery after photobleaching (FRAP). Photobleaching was performed for tau in tau/RNA droplets and tau/RNA/aSyn droplets (Figure 1d). Quantitative analysis showed that in both cases the fluorescence recovery was exponential and indistinguishable (Figure 1d; bottom). Similar results were obtained for the C-terminally truncated aSyn (Figure S2). The analysis showed that—without aging the sample—neither the mere presence of aSyn nor the concentration of aSyn inside the tau/RNA droplets slowed down the diffusion of tau.

2.5 | Ripening of tau/RNA/aSyn droplets

An intrinsic property of LLPS is the growth and fusion of liquid-like droplets with increasing incubation time. We therefore imaged the tau/RNA and tau/RNA/aSyn droplets immediately after preparation and again after 3 hr of incubation at room temperature. While immediately after preparation droplets with a diameter of ~1–5 μm were observed, a giant condensate/droplet with a diameter of ~50 μm was seen in case of tau/RNA LLPS after 3 hr of incubation (Figure 2a). In the presence of aSyn, condensates as large as ~100 μm diameter were even observed (Figure 2a). Notably, a strong enrichment of aSyn inside the growing tau/RNA droplets had occured (Figure 2b).

2.6 | Interplay of aSyn fibrils with preformed tau/RNA/aSyn droplets

To gain insight into the interplay between aSyn fibrils and tau condensates, we prepared tau/RNA droplets, into which aSyn was partitioned. Afterwards we added aSyn fibrils. This condition mimics a situation inside a neuron that contains tau condensates encountered by aSyn fibrils. The aSyn fibrils, for example, might have been taken up by the neuron as part of the trans-cellular spreading of aSyn inside the brain of a PDD patient. aSyn-containing tau droplets were observed by DIC and fluorescence microscopy in a freshly prepared sample (Figure 2c). Some of these tau/RNA/aSyn droplets were attached to aSyn fibrils (Figure 2c, left), whereas other aSyn fibrils remained separated/free (marked by asterisks in Figure 2c). After incubation for 1.5 hr at room temperature the droplets had increased in size (Figure 2c, right), presumably due to Ostwald ripening. In addition, some deformed tau/RNA droplets were observed (Figure 2c, right). The data show that aSyn fibrils can associate with tau/RNA droplets and change their morphology, thus providing support for a mechanism in which the perturbation of tau condensates by aSyn fibrils contributes to disease severity.

2.7 | Cdk2-phosphorylation of tau disfavors aSyn partitioning into tau droplets

Previous studies have shown that phosphorylation of tau by the proline-directed kinase Cdk2 promotes LLPS of tau in the absence of RNA.[24] NMR-based analysis furthermore showed that Cdk2 phosphorylates predominantly residues in the proline-rich region P2 of tau (Figure 3a).[24] We therefore tested if Cdk2-phosphorylation of tau enhances RNA-mediated LLPS of tau. Quantification of tau fluorescence intensities inside and outside of the droplets resulted in partition coefficients of ~3.3 and ~4.5 for unmodified and Cdk2-phosphorylated tau, respectively (Figure 3b, Table 1).

We then asked if aSyn or aSyn$^{\Delta C}$ partition into the droplets of Cdk2-phosphorylated tau. In agreement with the findings for unmodified tau, aSyn$^{\Delta C}$ was enriched very little inside pTau(Cdk2)/RNA droplets (Figure 3b,

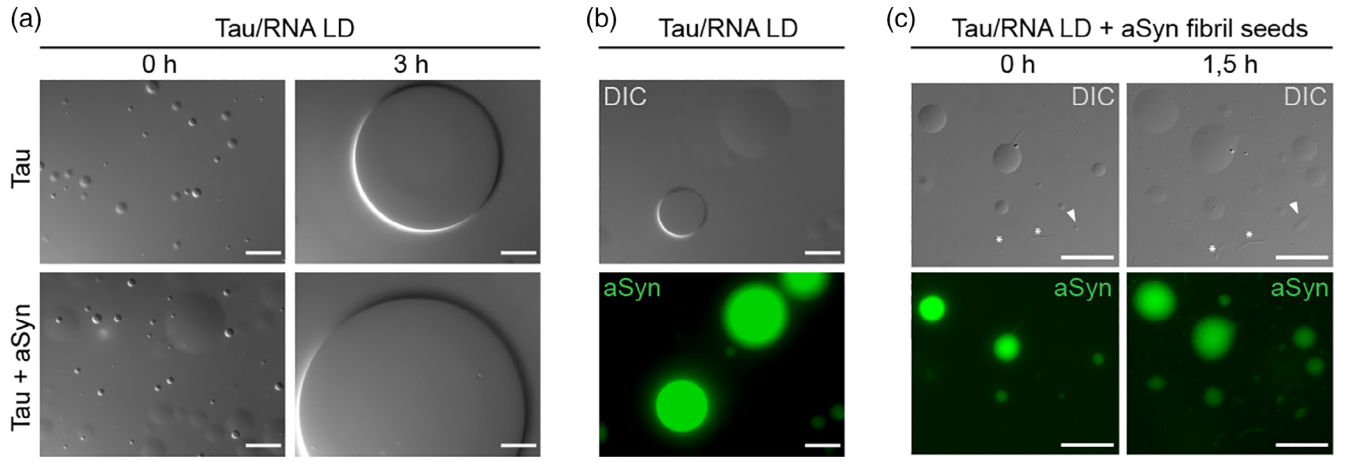

FIGURE 2 Ripening of tau + aSyn droplets. (a) Differential interference contrast microscopy (DIC) microscopy of tau/RNA liquid droplets of 60 μM tau control (upper panels) or 50 μM tau +10 μM aSyn (lower panels) prepared using 60 nM polyU and stabilized by addition of 2.5% dextran. Samples were imaged immediately after preparation or after 3 hr incubation at room temperature. (b) Giant droplets of 50 μM tau +10 μM aSyn spiked with a small amount of Alexa Fluor 488-labeled aSyn were prepared as described in (a) and imaged by DIC and fluorescence microscopy. Note the strong enrichment of fluorescently labeled aSyn in giant tau/RNA droplets. (c) Tau/RNA liquid droplets containing aSyn prepared as in (b) (i.e., with 60 nM polyU and 2.5% dextran) were mixed in an Eppendorf tube with freshly sonicated aSyn fibrils (final fibril concentration 5 μM). As in (b), the sample was spiked with a small amount of Alexa Fluor 488-labeled aSyn. Samples were imaged immediately after preparation (0 hr), and after 1.5 hr incubation at room temperature. White arrow—Droplets with deformed shape; white asterisk—aSyn fibrils. Scale bar, 20 μm

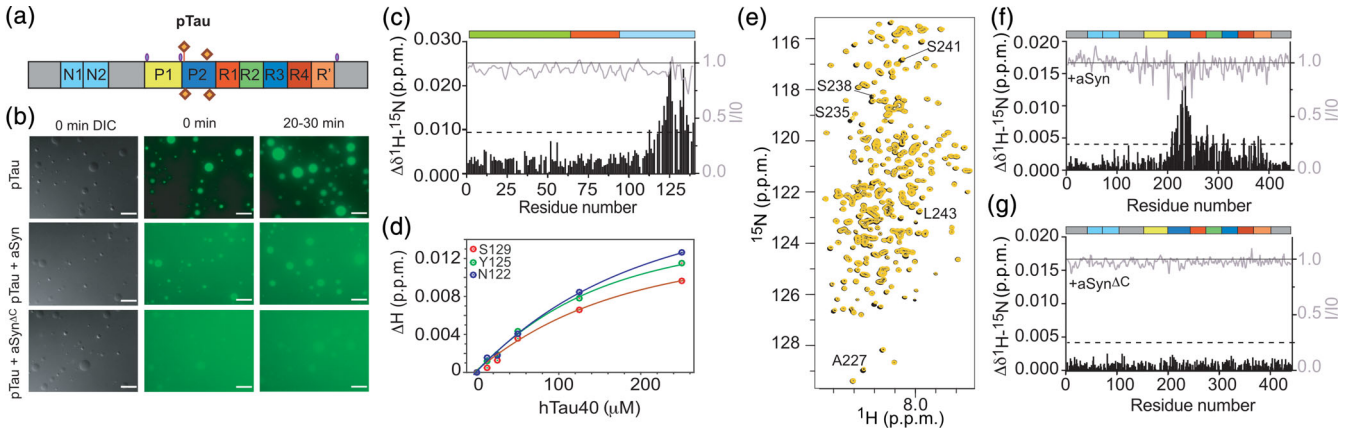

FIGURE 3 Interaction of aSyn with the proline-rich region P2 of tau. (a) Domain organization of 2N4R tau displaying the inserts N1 and N2, the two proline-rich regions P1 and P2 and the five pseudo-repeats R1-R4 and R′. Sites phosphorylated by Cdk2 are marked with diamonds (larger diamonds indicate more strongly phosphorylated sites).[24] (b) RNA-mediated LLPS of Cdk2-phosphorylated tau (top), and enrichment of aSyn in pTau(Cdk2)/RNA droplets (middle; Table 1). $aSyn^{\Delta C}$ was not significantly enriched in pTau(Cdk2)/RNA droplets (bottom; Table 1). Scale bars, 20 μm. Fluorescence images were taken immediately after addition of aSyn (middle) and after 20–30 min of incubation (right). (c) Normalized and averaged ^{1}H-^{15}N chemical shift perturbations (black bars; left axis) together with normalized signal intensity changes (gray line; right axis) in aSyn upon addition of tau (aSyn:tau 1:10 molar ratio). The horizontal dotted line indicates the average chemical shift perturbation plus one *SD*. I and I_0 are the intensities of ^{1}H-^{15}N cross peaks in the presence and absence of tau. The domain organization of aSyn is reported on the top with the N-terminal domain, the NAC region and the C-terminal domain shown in green, orange and light blue, respectively. (d) Best fit of proton chemical shift changes of representative aSyn residues experiencing fast chemical exchange due to tau binding. (e) ^{1}H-^{15}N SOFAST-HMQC spectrum of tau in the absence (black) and in the presence of a 10-fold molar excess of aSyn (yellow). Cross peaks with pronounced chemical shift perturbation are labeled. (f, g) Normalized and averaged ^{1}H-^{15}N chemical shift perturbations (black bars; left axis) together with normalized signal intensity changes (gray line; right axis) in tau upon addition of a 10-fold molar excess of aSyn (f) or $aSyn^{\Delta C}$ (g). I and I_0 are the intensities of ^{1}H-^{15}N cross peaks in the presence or absence of aSyn (f) or $aSyn^{\Delta C}$ (g). The horizontal dotted lines indicate the average chemical shift perturbation plus one *SD*. The domain organization of 2N4R tau is displayed on the top

bottom row; Table 1). In the case of full-length aSyn, however, Cdk2-phosphorylation of tau modulated the partitioning of aSyn: less aSyn was concentrated inside of pTau(Cdk2)/RNA droplets when compared to tau/RNA droplets (Table 1).

2.8 | The C-terminal domain of aSyn interacts with the proline-rich region P2 of tau

The above experiments indicate that the partitioning of aSyn into tau droplets is specific and depends on a direct interaction between aSyn and tau. Previous studies have shown that tau binds to the C-terminal domain of aSyn.[4,37,38] Less is however known about the binding sites in tau.

We therefore performed NMR titration experiments with tau and aSyn. In agreement with previous studies, addition of tau caused chemical shift perturbations predominantly in the C-terminal domain of aSyn (Figure 3c). Although we did not reach saturation, fitting of the $^{1}H/^{15}N$ chemical shift perturbations of N122, Y125 and S129 for increasing concentrations of tau to a single site binding model resulted in a dissociation constant of ~200 μM (Figure 3d).

Next we added aSyn to ^{15}N-labeled tau and recorded two-dimensional $^{1}H/^{15}N$ correlation spectra (Figure 3e). Comparison of the NMR spectra of tau in the absence and presence of aSyn revealed changes in peak position for a number of cross peaks. Sequence-specific assignment of the cross peaks revealed that the strongest signal perturbations occur for the tau residues located in the proline-rich region P2 including A227 and S235 (Figure 3e). Additional, smaller chemical shift perturbations were observed in the repeat region of tau (Figure 3f). In contrast, addition of the C-terminal truncated protein $aSyn^{\Delta C}$ did not influence the intensity or position of the $^{1}H/^{15}N$ cross peaks of tau (Figure 3g). The analysis shows that while aSyn can bind to the repeat domain of tau,[4,37] full-length aSyn preferentially interacts with the proline-rich region P2 of tau. The binding of the C-terminal domain of aSyn to the proline-rich region P2 further suggests that the interaction is predominantly electrostatic in nature: the highly negatively charged C-terminal domain of aSyn binds to the strongly positively charged P2 domain of tau.

3 | DISCUSSION

In the brain of patients diagnosed with PDD insoluble deposits of aSyn and tau are often present.[1,2] Consistent with a toxic interplay between these two pathologies, aSyn and tau synergistically promote their oligomerization and fibrillization in vitro, inside cells and in animal models of neurodegenerative disease.[3-11,39] Because LLPS of proteins has recently been suggested to be an important process in neurodegenerative diseases, we here investigated the interaction of aSyn with tau and the consequences on tau LLPS. Using a combination of LLPS assays and NMR spectroscopy we showed that full-length but not carboxy-terminally truncated aSyn concentrates inside tau droplets. This partitioning depends on the direct binding of the carboxy-terminal domain of aSyn to the proline-rich region P2 of tau and is regulated by tau phosphorylation.

The tau protein and different parts of it readily phase separate in solution in the presence of RNA.[22,26] In addition, the repeat region undergoes LLPS at pH values close to its pI.[21] 2N4R tau also phase separates in the absence of RNA or molecular crowding agents, when the ionic strength of the solution is low.[26,40] In contrast, we found that aSyn, as well as a C-terminally truncated version of aSyn, have low LLPS propensity at physiological pH and temperature. In addition, we did not observe the formation of aSyn droplets in the presence of RNA. This, however, does not exclude that aSyn is able to phase separate in solution and bind to membrane-less organelles in the cell. Indeed, a previous study has shown that low pH enables aSyn LLPS in vitro.[30]

Condensates in cells often contain a large number of proteins and RNA. At the same time, not all proteins play the same role in the biogenesis of condensates. Indeed, a number of studies have suggested that some proteins act as scaffold proteins, that is the LLPS of these proteins drives condensation, while other proteins are clients that are recruited to the condensate initiated by LLPS of scaffold proteins.[41] We showed that although aSyn has a low propensity for LLPS in solution, it efficiently concentrates inside tau droplets (Figure 1). The enrichment of aSyn in tau droplets depends on the direct interaction between the P2 region of tau and the C-terminal domain of aSyn as demonstrated by C-terminal truncation of aSyn and phosphorylation of the P2 region of tau (Figures 1 and 3). Because the C-terminus of aSyn is highly negatively charged while the non-phosphorylated P2 domain of tau is positively charged, the data also indicate that partitioning of aSyn into tau droplets is electrostatically driven. Besides changes in electrostatic interactions due to tau phosphorylation, structural changes induced by phosphorylation in the P2 region[42] might further contribute to the decreased partitioning of aSyn into droplets of phosphorylated tau (Figure 3b, Table 1). In addition, we found that aSyn fibrils can associate with tau droplets (Figure 2c). Taken together the data suggest that while tau may act as a scaffold protein for condensation in neurons, for example,

on microtubules,[28,29] aSyn can become enriched in these condensates through direct binding to tau.

Several previous studies investigated the co-aggregation of aSyn and tau both in vitro and in cells.[3-11,38,39] The in vitro experiments by Giasson et al.[3] are particularly interesting, because they used purified compounds and secondary effects can therefore be excluded. Indeed, Giasson et al. demonstrated that coincubation of tau and aSyn induced polymerization of both proteins. In addition, the authors performed immuno-electron microscopy with antibodies recognizing the two proteins as well as secondary antibodies conjugated to gold particles, in order to probe the composition of the fibrils formed by mixing aSyn and tau. The analysis showed that individual fibrils were mostly homopolymers, whereas a few fibrils were labeled with antibodies to both aSyn and tau. In addition, other fibrils were labeled in spatially separate domains with antibodies to either tau or aSyn, suggesting that these fibrils resulted from the end-to-end annealing of filaments formed solely by either aSyn or tau.[3] Using FRAP we found that bleached tau fluorescence inside of tau/RNA droplets recovered with the same rate in the absence and presence of aSyn (Figure 1). This showed that early after recruitment of aSyn, the tau/RNA/aSyn droplets have not yet changed their material properties. In addition, both tau/RNA and tau/RNA/aSyn droplets grew in size during 3 hr of incubation into giant phase separated compartments (Figure 2a,b), presumably due to Oswald ripening. In addition we found that the association of aSyn fibrils with preformed tau/RNA/aSyn droplets changed the droplet morphology (Figure 2c), indicating that transcellular spreading of aSyn fibrils in PDD might perturb tau condensates in neurons that take up aSyn fibrils.

The C-terminal domain of aSyn is known to interact with a number of binding partners including tau.[43] We demonstrate that the C-terminal domain of aSyn binds to the proline-rich region P2 of tau (Figure 3). The proline-rich region P2 is important for the tau-promoted assembly of tubulin into microtubules,[44] a process that is inhibited by Cdk2-phosphorylation.[24,45] In addition, it contributes to the interaction of tau with the molecular chaperone Hsp90.[46] RNA also binds to the positively charged P2 region of tau.[26] Thus, both aSyn and RNA bind to similar regions in tau. The observation that the addition of aSyn does not dissolve tau droplets indicates that the interaction of the P2 region with both aSyn and RNA is very dynamic and thus allows the P2 region to participate in both binding processes. Because the repeat domain of tau also interacts both aSyn (Figure 3) and RNA,[26] it provides additional binding sites for the simultaneous interaction with both binding partners.

The combined data provide the biophysical basis for a model in which the enrichment of α-synuclein in tau condensates contributes to the synergistic formation of α-synuclein/tau pathologies.

4 | MATERIALS AND METHODS

4.1 | Protein expression and purification

Tau and aSyn were recombinantly produced in BL21 (DE3) *Escherichia coli* cells (Novagen) as previously described.[44,47] $aSyn^{\Delta C}$ was prepared similar to full-length aSyn. However, due to the different pI, after ammonium sulfate precipitation the protein was dialyzed overnight in a buffer containing 25 mM TRIS, 0.02% NaN3, pH 7.0. After dialysis, the sample was applied to an anion exchange column (GE Healthcare Life Sciences, Mono S 5/50 GL) and eluted applying a salt gradient from 0 to 1 M NaCl. Buffer exchange was achieved by gel filtration. ^{15}N-labeled aSyn and $aSyn^{\Delta C}$ were produced growing the bacteria in M9 minimal media supplemented with $^{15}NH_4Cl$ as only source of nitrogen.

4.2 | aSyn fibril preparation

To mimic as closely as possible disease-relevant aSyn fibrils in our assays, we used aSyn fibrils amplified from brain tissue as described previously.[48] To this end, aSyn fibrils generated from the same PMCA product of the Parkinson's disease patient #1 as in Strohaker et al.[48] were used as aggregation seeds and added at a concentration of 0.5% (wt/wt) to 250 μM aSyn stock solution (50 mM HEPES, 100 mM NaCl, pH 7.4, 0.02% NaN_3) followed by water bath sonication for 2 min and subsequent aggregation under quiescent conditions in 1.5 ml Eppendorf cups in a ThermoScientific Heratherm incubator.

4.3 | DIC and fluorescence microscopy

Liquid droplet formation of protein samples was monitored by DIC and fluorescence microscopy. Samples were fluorescently labeled on lysine residues using Alexa Fluor 488 Microscale Protein Labeling Kit (Thermo Fisher Scientific, #A30006) according to the manufacturer's instructions. In all experiments, small amount of labeled protein, which is not sufficient to induce droplet formation by itself, was added to unlabeled protein to the final concentration indicated in the text. If not stated otherwise, tau phase separation was induced using RNA

analog polyuridylic acid (polyU; Sigma #P9528) to the final concentration of 60 nM and stabilized by addition of 2.5% of crowding agent dextran T500 (Pharmacosmos) in final assay buffer 25 mM HEPES pH 7.4, 2 mM DTT. The exception is Figure 1b where small amount of fluorescein (FAM)-labeled aSyn was used (final concentration 2 μM) and liquid droplets of 50 μM tau protein were prepared using 10% crowding agent dextran in 50 mM HEPES pH 7.4 containing 50 mM KCl and 1 mM DTT. For microscopy, 5–10 μl of samples were loaded onto glass slides, covered with ø 18 mm coverslips and imaged either immediately or after indicated time. DIC and fluorescent images were acquired on a Leica DM6 B microscope with a 63x objective (water immersion) and processed using FIJI software (NIH). If not stated otherwise, experiments were performed at room temperature.

4.4 | aSyn recruitment experiments

For aSyn co-recruitment experiments into liquid droplets of unmodified tau protein, samples contained 1:5 ratio of aSyn:tau (final concentrations: 50 μM tau in combination with 10 μM aSyn or aSyn$^{\Delta C}$) while the control contained only tau protein in 60 μM concentration to compensate for the possible crowding effect of aSyn addition. Small amounts of Alexa Fluor 488 lysine labeled aSyn or aSyn$^{\Delta C}$ (residues 1–107) were mixed with unlabeled aSyn or aSyn$^{\Delta C}$ proteins respectively to the final concentration of 10 μM and added to the 50 μM tau. Liquid droplets were formed in above mentioned way. Tau was visualized by addition of small amounts of Alexa Fluor 488 lysine labeled tau. Recruitment was followed by DIC and fluorescence microscopy as described.

Tau was phosphorylated through overnight incubation at 30°C with recombinant Cdk2/Cyclin A2 kinase (Sigma, #C0495). Phosphorylation was confirmed by mass spectrometry. Recruitment experiments were performed as described above using approximately 1:3 molar ratio of aSyn:pTau(Cdk2) (final concentrations: 32–34 μM pTau(Cdk2) in combination with 10 μM aSyn or aSyn$^{\Delta C}$) while the control contained only tau (37 μM).

4.5 | Partitioning coefficients

Partitioning coefficient calculations were done on samples prepared the same way as for co-recruitment experiments (see above). Fluorescent microscopy images were acquired on a Leica DM6 B microscope with a 63× objective (water immersion) and analyzed using FIJI software. Fluorescence intensity of labeled proteins located inside condensed liquid droplets or in the dispersed phase of the samples (background of the images) was measured using the ROI manager tool of FIJI software. Partitioning ratios of fluorescently labeled tau, aSyn or aSyn$^{\Delta C}$ into liquid droplets formed by either tau or pTau(Cdk2) with 60 nM polyU and 2.5% dextran are calculated as the average droplet fluorescence intensity based on 35 droplets per sample and the average background fluorescence intensity based on 35 same-sized ROI measurements per sample (7 microscopy images per sample, 5 droplets/background ROIs measured per image). Partitioning ratios were calculated separately for each microscopy image. For the co-recruitment into tau liquid droplets two independent experiments were performed resulting in a total amount of 60–70 droplets per sample (14 microscopy images). The final partitioning coefficients and their *SD* were calculated from the mean partitioning ratios of the microscopy images.

4.6 | Fluorescence recovery after photobleaching

The influence of aSyn or aSyn$^{\Delta C}$ on dynamics of tau molecules in the phase-separated state was investigated by FRAP analysis. As described above, tau phase separation was induced using 60 nM polyU RNA and droplets were stabilized by addition of 2.5% crowding agent dextran. Samples contained 1:5 ratio of aSyn:tau (final concentrations: 50 μM tau in combination with 10 μM aSyn or aSyn$^{\Delta C}$) while the control contained only tau protein in 60 μM final concentration to compensate for the possible crowding effect of aSyn addition. Small amounts of Alexa Fluor 488 lysine labeled tau were mixed with the unlabeled tau protein to the final tau concentration indicated above and followed during recovery recording. To minimize droplet movement, FRAP recordings were done after ~15 min, which is the time required for freshly formed droplets to settle down on the glass slide and become less mobile.

FRAP experiments were recorded on a Leica TCS SP8 confocal microscope using 63× objective (oil immersion) and 488 argon laser line. A circular region of ~4 μm in diameter was chosen in a region of homogenous fluorescence away from the droplet boundary and bleached with five iterations of full laser power. Recovery was imaged at low laser intensity (0.05%). Three hundred frames were recorded with one frame per 330 ms. Pictures were analyzed in FIJI software (NIH) and FRAP recovery curves were calculated using standard methods. Briefly, measured fluorescence was corrected for background fluorescence and FRAP signals were internally normalized to their mean value during the three frames before bleaching. After correction for acquisition bleaching, the

values were normalized to the first post-bleach value that is set to 0. Values were averaged from five recordings and the resulting FRAP curves ± *SD* were fitted to a single exponential model (one-phase decay).

4.7 | NMR spectroscopy

$^{1}H/^{15}N$ SOFAST-HMQC experiments[49] were recorded using a 800 MHz Bruker Avance NEO spectrometer equipped with a triple resonance cryoprobe. Experiments were acquired with protein in 50 mM NaPi, 2 mM DTT and 0.02% NaN_3, supplemented with 5% D_2O. Spectra were processed using Topspin 4.0.6 (Bruker) and analyzed with ccpnmr Analysis 2.4.2.[50]

$^{1}H/^{15}N$ SOFAST-HMQC experiments on ^{15}N-labeled tau and ^{15}N-labeled aSyn were recorded at 278 K and 288 K, respectively, with a recycle delay of 0.2 s and 2048 x 356 complex points for the ^{1}H and ^{15}N dimensions. During the titration the concentration of the labeled protein was kept constant at 14 μM and 25 μM for tau and aSyn, respectively. ^{15}N-labeled tau (^{15}N-labeled aSyn) was titrated with increasing amounts of unlabeled aSyn (tau) until 10-fold excess of the ligand was reached. Sequence specific assignment of tau and aSyn was previously reported (BMRB IDs 28065, 50701 and 6968).[51-56] The combined $^{1}H/^{15}N$ chemical shift perturbation was calculated according to $(((\delta_H)^2 + (\delta_N/5)^2)/2)1/2$.

Because predominantly chemical shift perturbations were observed for most resonances, that is, the binding process was fast on the NMR time scale, the global dissociation constant (K_d) was calculated by fitting the following equation to the experimental data using MATLAB (v. R2016b 9.1.0.441655, The MathWorks, Inc., Natick, MA):

$$\Delta H = \Delta H_{\max}\left(\frac{P_0 + x + K_d - \sqrt{(P_0 + x + K_d)^2 - 4P_0x}}{2P_0}\right) \quad (1)$$

ACKNOWLEDGMENTS

We thank Melanie Wegstroth (MPIBPC) for sample preparation. Markus Zweckstetter was supported by the *The Michael J. Fox Foundation for Parkinson's Research* (Grant ID: 16075) and the advanced grant "787679—LLPS-NMR" of the European Research Council.

AUTHOR CONTRIBUTIONS

Anna Siegert: Data curation; formal analysis; investigation; writing-review and editing. **Marija Rankovic:** Formal analysis; investigation; supervision; validation; visualization; writing-review and editing. **Filippo Favretto:** Formal analysis; investigation; writing-review and editing. **Tina Ukmar-Godec:** Formal analysis; investigation; writing-review and editing. **Timo Strohäker:** Resources. **Stefan Becker:** Investigation; resources; writing-review and editing.

CONFLICT OF INTEREST

The authors declare no potential conflict of interest.

DATA AVAILABILITY STATEMENT

All data that support the findings of this study are available from the corresponding authors upon reasonable request.

ORCID

Markus Zweckstetter https://orcid.org/0000-0002-2536-6581

REFERENCES

1. Yan X, Uronen RL, Huttunen HJ (2020) The interaction of alpha-synuclein and tau: A molecular conspiracy in neurodegeneration? Semin Cell Dev Biol 99:55–64.
2. Irwin DJ, Lee VM, Trojanowski JQ (2013) Parkinson's disease dementia: Convergence of alpha-synuclein, tau and amyloid-beta pathologies. Nat Rev Neurosci 14:626–636.
3. Giasson BI, Forman MS, Higuchi M, Golbe LI, Graves CL, Kotzbauer PT, Trojanowski JQ, Lee VM (2003) Initiation and synergistic fibrillization of tau and alpha-synuclein. Science 300:636–640.
4. Bhasne K, Sebastian S, Jain N, Mukhopadhyay S (2018) Synergistic amyloid switch triggered by early heterotypic oligomerization of intrinsically disordered alpha-synuclein and tau. J Mol Biol 430:2508–2520.
5. Badiola N, de Oliveira RM, Herrera F, Guardia-Laguarta C, Goncalves SA, Pera M, Suarez-Calvet M, Clarimon J, Outeiro TF, Lleo A (2011) Tau enhances alpha-synuclein aggregation and toxicity in cellular models of synucleinopathy. PLoS One 6:e26609.
6. Sengupta U, Guerrero-Munoz MJ, Castillo-Carranza DL, Lasagna-Reeves CA, Gerson JE, Paulucci-Holthauzen AA, Krishnamurthy S, Farhed M, Jackson GR, Kayed R (2015) Pathological interface between oligomeric alpha-synuclein and tau in synucleinopathies. Biol Psychiatry 78:672–683.
7. Esposito A, Dohm CP, Kermer P, Bahr M, Wouters FS (2007) Alpha-synuclein and its disease-related mutants interact differentially with the microtubule protein tau and associate with the Actin cytoskeleton. Neurobiol Dis 26:521–531.
8. Benussi L, Ghidoni R, Paterlini A, Nicosia F, Alberici AC, Signorini S, Barbiero L, Binetti G (2005) Interaction between tau and alpha-synuclein proteins is impaired in the presence of P301L tau mutation. Exp Cell Res 308:78–84.
9. Jensen PH, Hager H, Nielsen MS, Hojrup P, Gliemann J, Jakes R (1999) Alpha-synuclein binds to tau and stimulates the protein kinase A-catalyzed tau phosphorylation of serine residues 262 and 356. J Biol Chem 274:25481–25489.
10. Roy B, Jackson GR (2014) Interactions between tau and alpha-synuclein augment neurotoxicity in a drosophila model of Parkinson's disease. Hum Mol Genet 23:3008–3023.
11. Guo JL, Covell DJ, Daniels JP, Iba M, Stieber A, Zhang B, Riddle DM, Kwong LK, Xu Y, Trojanowski JQ, Lee VM (2013)

Distinct alpha-synuclein strains differentially promote tau inclusions in neurons. Cell 154:103–117.
12. Chong PA, Forman-Kay JD (2016) Liquid-liquid phase separation in cellular signaling systems. Curr Opin Struct Biol 41: 180–186.
13. Hyman AA, Weber CA, Julicher F (2014) Liquid-liquid phase separation in biology. Annu Rev Cell Dev Biol 30:39–58.
14. Aguzzi A, Altmeyer M (2016) Phase separation: Linking cellular compartmentalization to disease. Trends Cell Biol 26: 547–558.
15. Patel A, Lee HO, Jawerth L, Maharana S, Jahnel M, Hein MY, Stoynov S, Mahamid J, Saha S, Franzmann TM, Pozniakovski A, Poser I, Maghelli N, Royer LA, Weigert M, Myers EW, Grill S, Drechsel D, Hyman AA, Alberti S (2015) A liquid-to-solid phase transition of the ALS protein FUS accelerated by disease mutation. Cell 162:1066–1077.
16. Taylor JP, Brown RH Jr, Cleveland DW (2016) Decoding ALS: From genes to mechanism. Nature 539:197–206.
17. Monahan Z, Ryan VH, Janke AM, Burke KA, Rhoads SN, Zerze GH, O'Meally R, Dignon GL, Conicella AE, Zheng W, Best RB, Cole RN, Mittal J, Shewmaker F, Fawzi NL (2017) Phosphorylation of the FUS low-complexity domain disrupts phase separation, aggregation, and toxicity. EMBO J 36: 2951–2967.
18. Boeynaems S, Bogaert E, Kovacs D, Konijnenberg A, Timmerman E, Volkov A, Guharoy M, De Decker M, Jaspers T, Ryan VH, Janke AM, Baatsen P, Vercruysse T, Kolaitis RM, Daelemans D, Taylor JP, Kedersha N, Anderson P, Impens F, Sobott F, Schymkowitz J, Rousseau F, Fawzi NL, Robberecht W, Van Damme P, Tompa P, Van Den Bosch L (2017) Phase separation of C9orf72 dipeptide repeats perturbs stress granule dynamics. Mol Cell 65:1044–1055.
19. Molliex A, Temirov J, Lee J, Coughlin M, Kanagaraj AP, Kim HJ, Mittag T, Taylor JP (2015) Phase separation by low complexity domains promotes stress granule assembly and drives pathological fibrillization. Cell 163:123–133.
20. Conicella AE, Zerze GH, Mittal J, Fawzi NL (2016) ALS mutations disrupt phase separation mediated by alpha-helical structure in the TDP-43 low-complexity C-terminal domain. Structure 24:1537–1549.
21. Ambadipudi S, Biernat J, Riedel D, Mandelkow E, Zweckstetter M (2017) Liquid-liquid phase separation of the microtubule-binding repeats of the Alzheimer-related protein tau. Nat Commun 8:275.
22. Zhang X, Lin Y, Eschmann NA, Zhou H, Rauch JN, Hernandez I, Guzman E, Kosik KS, Han S (2017) RNA stores tau reversibly in complex coacervates. PLoS Biol 15:e2002183.
23. Wegmann S, Eftekharzadeh B, Tepper K, Zoltowska KM, Bennett RE, Dujardin S, Laskowski PR, MacKenzie D, Kamath T, Commins C, Vanderburg C, Roe AD, Fan Z, Molliex AM, Hernandez-Vega A, Muller D, Hyman AA, Mandelkow E, Taylor JP, Hyman BT (2018) Tau protein liquid-liquid phase separation can initiate tau aggregation. EMBO J 37:e98049.
24. Savastano A, Flores D, Kadavath H, Biernat J, Mandelkow E, Zweckstetter M (2021) Disease-associated tau phosphorylation hinders tubulin assembly within tau condensates. Angew Chem Int Ed Engl 60:726–730.
25. Ferreon JC, Jain A, Choi KJ, Tsoi PS, MacKenzie KR, Jung SY, Ferreon AC (2018) Acetylation disfavors tau phase separation. Int J Mol Sci 19:1360.
26. Ukmar-Godec T, Hutten S, Grieshop MP, Rezaei-Ghaleh N, Cima-Omori MS, Biernat J, Mandelkow E, Soding J, Dormann D, Zweckstetter M (2019) Lysine/RNA-interactions drive and regulate biomolecular condensation. Nat Commun 10:2909.
27. Hernandez-Vega A, Braun M, Scharrel L, Jahnel M, Wegmann S, Hyman BT, Alberti S, Diez S, Hyman AA (2017) Local nucleation of microtubule bundles through tubulin concentration into a condensed tau phase. Cell Rep 20:2304–2312.
28. Tan R, Lam AJ, Tan T, Han J, Nowakowski DW, Vershinin M, Simo S, Ori-McKenney KM, McKenney RJ (2019) Microtubules gate tau condensation to spatially regulate microtubule functions. Nat Cell Biol 21:1078–1085.
29. Siahaan V, Krattenmacher J, Hyman AA, Diez S, Hernandez-Vega A, Lansky Z, Braun M (2019) Kinetically distinct phases of tau on microtubules regulate kinesin motors and severing enzymes. Nat Cell Biol 21:1086–1092.
30. Ray S, Singh N, Kumar R, Patel K, Pandey S, Datta D, Mahato J, Panigrahi R, Navalkar A, Mehra S, Gadhe L, Chatterjee D, Sawner AS, Maiti S, Bhatia S, Gerez JA, Chowdhury A, Kumar A, Padinhaeeri R, Riek R, Krishnamoorthy G, Maji SK (2020) α-Synuclein aggregation nucleates through liquid–liquid phase separation. Nat Chem 12:705–716.
31. Oueslati A, Fournier M, Lashuel HA (2010) Role of post-translational modifications in modulating the structure, function and toxicity of alpha-synuclein: Implications for Parkinson's disease pathogenesis and therapies. Prog Brain Res 183:115–145.
32. Zhang Z, Kang SS, Liu X, Ahn EH, Zhang Z, He L, Iuvone PM, Duong DM, Seyfried NT, Benskey MJ, Manfredsson FP, Jin L, Sun YE, Wang JZ, Ye K (2017) Asparagine endopeptidase cleaves alpha-synuclein and mediates pathologic activities in Parkinson's disease. Nat Struct Mol Biol 24:632–642.
33. Chong PA, Vernon RM, Forman-Kay JD (2018) RGG/RG motif regions in RNA binding and phase separation. J Mol Biol 430: 4650–4665.
34. Roden C, Gladfelter AS (2020) RNA contributions to the form and function of biomolecular condensates. Nat Rev Mol Cell Biol, 10, 2020 Jul 6. https://doi.org/10.1038/s41580-020-0264-6
35. Wang Y, Mandelkow E (2016) Tau in physiology and pathology. Nat Rev Neurosci 17:5–21.
36. Cruz A, Verma M, Wolozin B (2019) The pathophysiology of tau and stress granules in disease. Adv Exp Med Biol 1184:359–372.
37. Lu J, Zhang S, Ma X, Jia C, Liu Z, Huang C, Liu C, Li D (2020) Structural basis of the interplay between alpha-synuclein and tau in regulating pathological amyloid aggregation. J Biol Chem 295:7470–7480.
38. Dasari AKR, Kayed R, Wi S, Lim KH (2019) Tau interacts with the C-terminal region of alpha-synuclein, promoting formation of toxic aggregates with distinct molecular conformations. Biochemistry 58:2814–2821.
39. Waxman EA, Giasson BI (2011) Induction of intracellular tau aggregation is promoted by alpha-synuclein seeds and provides novel insights into the hyperphosphorylation of tau. J Neurosci 31:7604–7618.
40. Boyko S, Qi X, Chen TH, Surewicz K, Surewicz WK (2019) Liquid-liquid phase separation of tau protein: The crucial role of electrostatic interactions. J Biol Chem 294:11054–11059.
41. Banani SF, Rice AM, Peeples WB, Lin Y, Jain S, Parker R, Rosen MK (2016) Compositional control of phase-separated cellular bodies. Cell 166:651–663.

42. Schwalbe M, Kadavath H, Biernat J, Ozenne V, Blackledge M, Mandelkow E, Zweckstetter M (2015) Structural impact of tau phosphorylation at threonine 231. Structure 23:1448–1458.
43. Lassen LB, Reimer L, Ferreira N, Betzer C, Jensen PH (2016) Protein partners of alpha-synuclein in health and disease. Brain Pathol 26:389–397.
44. Gustke N, Trinczek B, Biernat J, Mandelkow EM, Mandelkow E (1994) Domains of tau protein and interactions with microtubules. Biochemistry 33:9511–9522.
45. Amniai L, Barbier P, Sillen A, Wieruszeski JM, Peyrot V, Lippens G, Landrieu I (2009) Alzheimer disease specific phosphoepitopes of tau interfere with assembly of tubulin but not binding to microtubules. FASEB J 23:1146–1152.
46. Karagoz GE, Duarte AM, Akoury E, Ippel H, Biernat J, Moran Luengo T, Radli M, Didenko T, Nordhues BA, Veprintsev DB, Dickey CA, Mandelkow E, Zweckstetter M, Boelens R, Madl T, Rudiger SG (2014) Hsp90-tau complex reveals molecular basis for specificity in chaperone action. Cell 156:963–974.
47. Hoyer W, Antony T, Cherny D, Heim G, Jovin TM, Subramaniam V (2002) Dependence of alpha-synuclein aggregate morphology on solution conditions. J Mol Biol 322: 383–393.
48. Strohaker T, Jung BC, Liou SH, Fernandez CO, Riedel D, Becker S, Halliday GM, Bennati M, Kim WS, Lee SJ, Zweckstetter M (2019) Structural heterogeneity of alpha-synuclein fibrils amplified from patient brain extracts. Nat Commun 10:5535.
49. Schanda P, Kupce E, Brutscher B (2005) SOFAST-HMQC experiments for recording two-dimensional heteronuclear correlation spectra of proteins within a few seconds. J Biomol NMR 33:199–211.
50. Vranken WF, Boucher W, Stevens TJ, Fogh RH, Pajon A, Llinas M, Ulrich EL, Markley JL, Ionides J, Laue ED (2005) The CCPN data model for NMR spectroscopy: Development of a software pipeline. Proteins 59:687–696.
51. Bermel W, Bertini I, Felli IC, Lee YM, Luchinat C, Pierattelli R (2006) Protonless NMR experiments for sequence-specific assignment of backbone nuclei in unfolded proteins. J Am Chem Soc 128:3918–3919.
52. Bertoncini CW, Jung YS, Fernandez CO, Hoyer W, Griesinger C, Jovin TM, Zweckstetter M (2005) Release of long-range tertiary interactions potentiates aggregation of natively unstructured alpha-synuclein. Proc Natl Acad Sci USA 102:1430–1435.
53. Narayanan RL, Durr UH, Bibow S, Biernat J, Mandelkow E, Zweckstetter M (2010) Automatic assignment of the intrinsically disordered protein tau with 441-residues. J Am Chem Soc 132:11906–11907.
54. Mukrasch MD, Bibow S, Korukottu J, Jeganathan S, Biernat J, Griesinger C, Mandelkow E, Zweckstetter M (2009) Structural polymorphism of 441-residue tau at single residue resolution. PLoS Biol 7:e34.
55. Ukmar-Godec T, Fang P, Ibanez de Opakua A, Henneberg F, Godec A, Pan KT, Cima-Omori MS, Chari A, Mandelkow E, Urlaub H, Zweckstetter M (2020) Proteasomal degradation of the intrinsically disordered protein tau at single-residue resolution. Sci Adv 6:eaba3916.
56. Mukrasch MD, von Bergen M, Biernat J, Fischer D, Griesinger C, Mandelkow E, Zweckstetter M (2007) The "jaws" of the tau-microtubule interaction. J Biol Chem 282:12230–12239.

SUPPORTING INFORMATION

Additional supporting information may be found online in the Supporting Information section at the end of this article.

How to cite this article: Siegert A, Rankovic M, Favretto F, et al. Interplay between tau and α-synuclein liquid–liquid phase separation. *Protein Science*. 2021;1–11. https://doi.org/10.1002/pro.4025